Typeset with jjap2.cls <ver.1.0> **Regular Paper**

Effects of Dissolved and Ambient Gases on Sonochemical Degradation of Methylene Blue in High-Amplitude Resonant Mode

Hirotsugu OGI, Yusuke TOMIYAMA, Yusuke SHOJI, Tomoo MIZUGAKI and Masahiko HIRAO

Graduate School of Engineering Science, Osaka University, 1-3 Machikaneyama, Toyonaka, Osaka 560-8531, Japan

In this paper, we show the dominant contribution of an ambient gas to sonochemical reactions in a high-amplitude acoustic resonant mode. A high-amplitude resonant mode in the solution was predicted by the three-layer resonator model, which showed an acoustic amplitude higher than the standard amplitude by a factor of 5. The high-amplitude resonance mode was used to decompose methylene blue in water. The effects of the dissolved gases and the ambient gases of argon, oxygen, and helium on the degradation efficiency were systematically studied using a closed resonant reactor. The maximum efficiency was achieved when the ambient gas was argon regardless of the dissolved gases. The replacement of dissolved gas with ambient gas is enhanced with high-amplitude ultrasonic irradiation.

KEYWORDS: sonochemistry, methylene blue, resonance, decomposition, ambient gas, dissolved gas

1. Introduction

Irradiation of an aqueous solution with ultrasonic waves causes cavitation bubbles, which repeatedly grow and collapse in synchrony with the driving acoustic pressure. When bubbles collapse, the temperature inside bubbles drastically increases, providing hot spots and free radial species that decompose organic compounds in the solution,[1–3] that is, the sonochemical reaction. Sonochemical reactions have been the object of intense studies and two principal mechanisms have been indicated. The first is the pyrolysis mechanism occurring near the hot spots.[4,5] The other is the decomposition by the radical species, mainly OH and H radicals formed by the dissociation of water.[6] These sonochemical reactions are highly affected by dissolved gases and hence their influence was studied.[7–9] Ambient gases also significantly affect the sonochemical reactions because ultrasonic irradiation tends to accelerate the attainment of the solubility equilibrium as indicated by Hart and Henglein[10] and Harada and Kumagai[11] in their studies on the H_2O_2 production rate in water. Recently, high-power acoustic methods are being adopted in sonochemical reactions, and the effects of dissolved and ambient gases on sonochemical reactions must be studied systematically.

Here we investigate their effects on the efficiency of sonochemical decomposition in a high-amplitude resonance mode. The examined organic compound is methylene blue (MB), which is a typical dyestuff that cannot be degraded by a conventional method such as biological

treatment. Photocatalytic degradation of MB has been achieved by irradiating a solution containing MB and TiO_2 powder with ultraviolet light.[12,13] The principal decomposition mechanism of MB in the photocatalytic method is oxidation of substances by OH radicals. The sonochemical degradation of MB will proceed with oxidation by the radical species and pyrolysis reactions. The separation of their contributions is not straightforward, but both mechanisms originate from the high-temperature fields caused by cavitation bubbles. Because the species of dissolved gases govern the thermodynamics of bubbles, the decomposition efficiency can be a measure for evaluating the effect of the gases.

We recently showed that there are high-amplitude resonant modes in the reactor for sonochemistry composed of three layers[14] and that the acoustic amplitude in the solution is extremely sensitive to the height of the solution in the reactor. Here, we confirm the theory and show the importance of using a high-amplitude resonance mode in sonochemical reactions. Throughout this study, we used the high-amplitude resonant mode to achieve efficient decomposition of MB in water.

2. High-Amplitude Resonant Modes

Ultrasonic plane waves generated by the transducer cause the three-layer resonance modes in our resonance reactor, as shown later. They are the solution layer (layer 3), the glass layer of the bottom at the reactor container (layer 2), and the cooling-water layer between the transducer and the reactor (layer 1). Previously, we showed that there are high-amplitude and low-amplitude resonant modes in such a three-layer resonator[14,15] and we derived the frequency equation:

$$\tan\eta + \zeta\frac{\delta_1\cos\gamma + \delta_2\sin\gamma}{\delta_2\cos\gamma - \delta_1\sin\gamma} = 0. \tag{1}$$

Here, $\eta = k_3 d_3$, $\gamma = k_2(d_1 + d_2)$, and $\zeta = k_2 C_2/(k_3 C_3)$, where d_i, C_i, and k_i denote the thickness, the longitudinal-wave modulus and the wavenumber for the ith layer, respectively. $\delta_1 = \zeta_1\cos\alpha\cos\beta + \sin\alpha\sin\beta$, $\delta_2 = \zeta_1\cos\alpha\sin\beta - \sin\alpha\cos\beta$, and $\zeta_1 = C_1 k_1/(C_2 k_2)$. Analysis with eq. (1) shows that the high-amplitude modes are very sensitive to the height of the solution in the reactor (d_3), as shown in Fig. 1, indicating that we must carefully determine the height of the solution in the sonochemical decomposition when we use cooling water between the transducer and the reactor. Figure 2 shows examples of the amplitude distributions for high-amplitude and low-amplitude resonant modes. The high-amplitude mode realizes a much higher amplitude in the solution layer than does the low-amplitude mode by a factor of 5.

We measure the acoustic amplitude in the reactor, shown later in detail, along the vertical direction to confirm our modal analysis. We pour distilled water in the reactor until the height reaches a target d_3 value. We adjust the distance between the reactor and the transducer (d_1) to find the resonance state by measuring the amplitude with a PZT detector (thickness 0.5

mm and diameter 3 mm). The maximum amplitude was detected by moving the detector vertically. Thus, a set of d_1 and d_3 is obtained, which gives a resonance state. We changed the d_3 value to determine the amplitude dependence on d_3. The results, shown in Fig. 3, provide the following observations. (i)The maximum amplitude in the reactor varies by a factor of 2, depending on d_3, despite the fact that we adjust d_1 at each d_3 to obtain the maximum amplitude. (ii) Dependences of the amplitude and d_1 on d_3 agree with those predicted by the calculation. (iii) The difference between the maximum and minimum amplitudes measured is smaller than that predicted. This principally occurs because we do not consider dissipation factors such as heat loss.

Quantitative discrepancies between measurements and calculations appear because we use a simple model of linear and one-dimensional plane-wave resonance and disregard radial displacement and the nonlinearity of water. However, the view that the combination of d_1 and d_3 strongly affects the amplitude inside the reactor is essential.

For further confirmation, we measured the amount of decomposed MB in water by changing d_3 and compared the result with the predicted amplitude, as shown in Fig. 4. The degradation efficiency changes depending on d_3 despite the optimized d_1, and this dependence on d_3 corresponds to the dependence of the calculated amplitude. These analytical results and supporting measurements strongly suggest the importance of controlling the amount of solution in sonochemical reactions. Thus, we carefully determined the dimensions of our resonator system and used the high-amplitude modes throughout this study. The frequency of the ultrasonic wave was 200 kHz.

3. Measurement Setup

Figure 5 shows our measurement system. A cylindrical Pyrex-glass reactor (capacity: 500 ml, inner diameter: 70 mm, height: 160 mm, bottom thickness: 3 mm) was placed into ice-cold water. Beneath the reactor, a piezoelectric transducer was installed to irradiate the reactor's bottom surface with the longitudinal plane wave. The distance between the transducer and the reactor (d_1) was adjustable by moving the stage, and a suitable distance was set to achieve the high-amplitude resonant mode. A 500 ml container for preparing a gas-saturated liquid is connected via a Teflon tube. A fiber-membrane degassing module is connected to the container to supply degassed distilled water. Degasification was accomplished by evacuating gases from the input distilled water through the fiber membrane, using a rotary pump; the concentration of dissolved oxygen (DO) in the treated water was less than 0.5 mg/l (initial concentration was about 5 mg/l).

We show the procedure of the measurement below.

(1) Inject a 10 ml MB solution with the MB concentration of 100 ppm into the reactor.
(2) Evacuate the air from the reactor using the rotary pump.
(3) Supply the reactor with the target ambient gas and then evacuate the gas. We repeat this

procedure three times to exchange the air with the target ambient gas. Then, we evacuate the gas to make the pressure lower inside the reactor.

(4) Replace the air in the gas-saturation container with the target dissolving gas three times using the rotary pump and supply the container with the water degassed through the membrane module by connecting it to the rotary pump.

(5) Bubble the degassed water with the dissolving gas for 30 min to prepare the gas-saturated water.

(6) Transport the gas-saturated water from the container to the reactor through the Teflon tube by increasing the pressure of the dissolving gas in the container.

(7) Inundate the reactor atmosphere with the target ambient gas and irradiate the reactor with ultrasonic waves.

The initial concentration of MB before ultrasonic irradiation was 10 ppm and the total amount of solution was 100 ml. The irradiation time was 15 min. Target gases were argon, oxygen, and helium.

The concentration of MB in the irradiated solution was determined using a spectrophotometer. Figure 6 (a) shows the calibration measurement to relate the absorbance with the concentration of MB. The representative absorbance at 665 nm was used. Figure 6 (b) shows the typical change of the absorbance spectrum before and after the ultrasonic irradiation for 15 min.

4. Results and Discussion

We investigated the effects of the dissolved gas and the ambient gas by comparing the degradation efficiency among the eight cases shown in Fig. 7. The combinations of ambient gas/dissolved gas are (a) Ar/Ar, (b) O_2/O_2, (c) He/He, (d) Ar/degassed, (e) O_2/degassed, (f) Ar/O_2, (g) O_2/Ar, and (h) vacuum/Ar. To check the reproducibility, we made three independent measurements for each case.

Figure 8 shows the results. We did not include the result for case (h) in the figure because of its very low value; the amount of decomposed MB was less than 1 ppm.

First, we note cases (a), (b), and (c), in which the same gases are used in the solution and atmosphere. The degradation efficiency was the highest for Ar/Ar, the next highest for O_2/O_2, and the lowest for He/He. This trend is related with the thermal conductivity, specific heat, and solubility of these gases. Their standard values are shown in Table I. It is widely recognized that the temperature inside a bubble when it collapses strongly depends on the specific heat because of nearly adiabatic volume change of the bubble; higher specific heat causes a greater increase of the temperature inside the bubble at the time of collapse. Thermal conductivity will determine the degree of the adiabatic compression; higher thermal conductivity will cause the thermal energy inside the bubble to leak into the bulk liquid, suppressing the increase

of the hot-spot temperature. The solubility of the gas determines the contribution of the gas to the thermal properties with the bubble dynamics. Helium shows a large specific heat, the highest thermal conductivity, and the lowest solubility. The lowest degradation efficiency is, therefore, associated with its high thermal conductivity and low solubility.

As reported previously,[16,17] oxygen atoms enhance the formation of OH radicals, and the degradation efficiency in case (b) would be higher provided the oxidation by OH radicals is principal degradation mechanism of MB. The lower degradation efficiency with oxygen therefore suggests that the principal mechanism is the pyrolysis degradation. Actually, argon shows a lower thermal conductivity than that of oxygen by a factor of 1.5, indicating a higher temperatures upon the bubble collapsed because of adiabatic compression. After the collapse, the hot spot increases the temperature of the surrounding liquid.

Next, we discuss the replacement of the dissolved gas with the ambient gas. Figure 8 shows the important result that the degradation efficiency can be high when the ambient gas is Ar [cases (a), (d), and (f)], regardless of the gas dissolved in the solution. For the O_2-saturated solution [case (f)], for example, the degradation efficiency was as high as that in the case of Ar/Ar. On the other hand, it was lower when the ambient gas was O_2, even when Ar was saturated before irradiation [case (g)]. These indicate the replacement of the dissolved gas with the ambient gas. We measured the amount of dissolved oxygen (DO) before and after the ultrasonic irradiation for cases (f) and (g) using a DO meter (resolution: 0.01 mg/l, Horiba). As shown in Table II, the gas in the solution is replaced with that in the ambient after the irradiation. According to Henry's law, the concentration of a solute gas in a solution is proportional to the partial pressure of the gas in the atmosphere. Because initial partial pressures of the dissolved gases in cases (f) and (g) are nearly zero, replacement between dissolved and ambient gases naturally occurs within a certain time. Degasification upon ultrasonic irradiation accelerated this replacement. Thus, ambient gas has the most significant effect on sonochemical reactions rather than the initial dissolved gas in the high-acoustic-amplitude mode even for a short irradiation time.

The lowered degradation efficiency when the solution is degassed [case (d) or (e)] is attributed to a decreased amount of dissolved gas. Ultrasonic irradiation will make the solution absorb the ambient gas but the ambient pressure decreases during this process, leading to the total amount of the dissolved gas being smaller than that in the initial gas-saturated solution. The extremely low degradation efficiency in case (h) is therefore explained by the quick degasification of the solute gas atoms into the atmosphere.

5. Conclusions

First, the high-amplitude resonance mode predicted by the three-layer model was confirmed by measuring the amplitude dependence on the height of the solution in the reactor and by the dependence of the degradation efficiency on the solution height. These results

strongly indicated that the sonochemical reaction is very sensitive to the height of the solution.

Second, the effects of dissolved and ambient gases on sonochemical degradation of methylene blue were systematically investigated in a closed resonant system in the high-amplitude mode. The examined gases were argon, oxygen, and helium. The high-amplitude resonance mode was adopted throughout the degradation. The dissolved gases were quickly replaced with the ambient gas under high-amplitude ultrasonic irradiation, and the ambient gas showed the most significant influence on the degradation measurement. Thus, before discussing the effect of the dissolved gases on a sonochemical reaction, control of the pressure and volume of the ambient gas is indispensable.

References

1) J. Dewulf, H. Langenhove, A. Visscher and S. Sabbe: Ultrason. Sonochem. **8** (2001) 143.

2) L. Rong, K. Yasuda, Y. Bando and M. Nakamura: Jpn. J. Appl. Phys. **41** (2002) 3272.

3) A. Colussi, H. Ming Hung, and M. Hoffmann: J. Phys. Chem. A **103** (1999) 2696.

4) M. Fitzgerald, V. Griffing and J. Sullivan: J. Chem. Phys. **25** (1956) 926.

5) K. Suslick, D. Hammerton and R. Cline: J. Am. Chem. Soc. **108** (1986) 5641.

6) V. Misik, N. Miyoshi, and P. Riesz: J. Phys. Chem. **99** (1995) 3605.

7) Y. Kojima, T. Fujita, E. Ona, H. Matsuda, S. Koda, N. Tanahashi and Y. Asakura: Ultrason. Sonochem. **12** (2005) 359.

8) D. Wayment and D. Casadonte: Ultrason. Sonochem. **9** (2002) 251.

9) J. Berlan, F. Trabelsi, H. Delmas, A. Wilhelm and J. Petrignani: Ultrason. Sonochem. **1** (1994) S97.

10) E. Hart and A. Henglein: J. Phys. Chem. **89** (1985) 4342.

11) H. Harada and H. Kumagai: Jpn. J. Appl. Phys. **42** (2003) 2958.

12) A. Mills and J. Wang: J. Photochem. Photobiol. A **127** (1999) 123.

13) T. Zhang, T. Oyama, A. Aoshima, H. Hidaka, J. Zhao and N. Serpone: J. Photochem Photobiol. A **140** (2001) 163.

14) Y. Tomiyama, H. Ogi, F. Muramatsu and M. Hirao: presented at 5th Int. Symp. Cav. (CAV 2003), Osaka, Japan, Nov. 1-4, 2003.

15) H. Ogi, G. Shimoike, M. Hirao, K. Takashima and Y. Higo: J. Appl. Phys. **91** (2002) 4857.

16) M. Kubo, K. Matsuoka, A. Takahashi, N. Shibasaki-Kitakawa and T. Yonemoto: Jpn. J. Appl. Phys. **12** (2005) 263.

17) A. Colussi, L. Weavers, and M. Hoffmann: J. Phys. Chem. A **102** (1998) 6927.

Table I. Thermal conductivity (273 K), specific heat, and solubility (293 K) of gases.

	Thermal conductivity (10^{-2}W m^{-1} K^{-1})	Specific heat	Solubility (cm^3/cm^3)
Air	2.41	1.403	0.019
O_2	2.45	1.396	0.031
N_2	2.40	1.405	0.016
Ar	1.63	1.67	0.035
He	14.22	1.66	0.0088

Table II. Measured DO (mg/L) before and after ultrasonic irradiation for cases (f) and (g).

	Before	After
Case (f)	>40	1.15
Case (g)	1.09	>20

Figure Caption

Fig. 1 Dependence of the normalized acoustic-pressure amplitude in the solution R_p (ratio of the amplitude in the solution layer (layer 3) to that in the cooling-water layer (layer 1) on the height of the solution layer d_3 at the frequency of 200 kHz.

Fig. 2 Distributions of normalized acoustic pressure along the propagation direction of the ultrasonic plane wave in the (a) high-amplitude mode and (b) low-amplitude mode.

Fig. 3 (a) Measured dependence of the acoustic amplitude and that of the corresponding d_1 on d_3. (b) Dependences of R_p and d_1 on d_3 calculated using the three-layer model. The origin of the horizontal axis is parallel-shifted in (a) so as to obtain the maximum amplitude between the measurement and calculations at the same position.

Fig. 4 Dependences of (a) R_p and (b) the degradation efficiency of MB (fraction of the amount of decomposed MB to the initial value) on d_3. The initial MB concentration was 10 ppm and the ultrasonic power was 23 W.

Fig. 5 Setup of the sonochemical degradation of methylene blue in a closed resonance reactor.

Fig. 6 (a) Calibration measurement for quantitative determination of concentration of methylene blue in water. (b) Typical absorbance spectra before and after ultrasonic irradiation.

Fig. 7 Eight cases of degradation measurement with various dissolved gases and ambient gases.

Fig. 8 Amount of decomposed MB upon ultrasonic irradiation for seven of the cases shown in Fig.7.

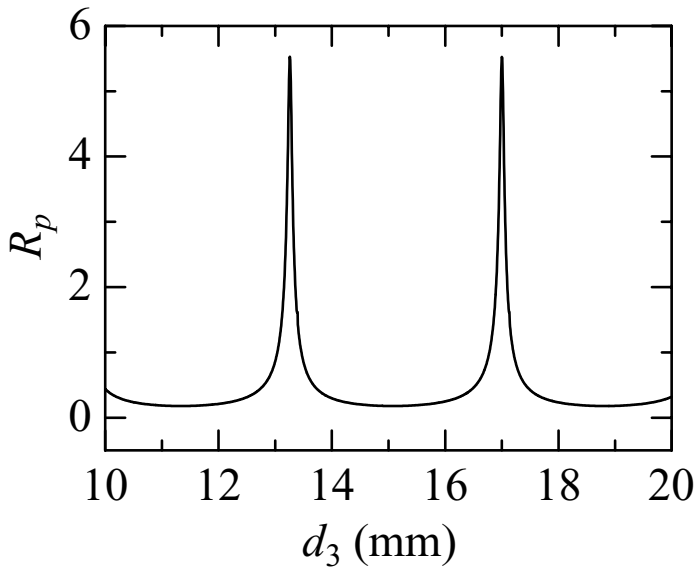

Fig. 1.

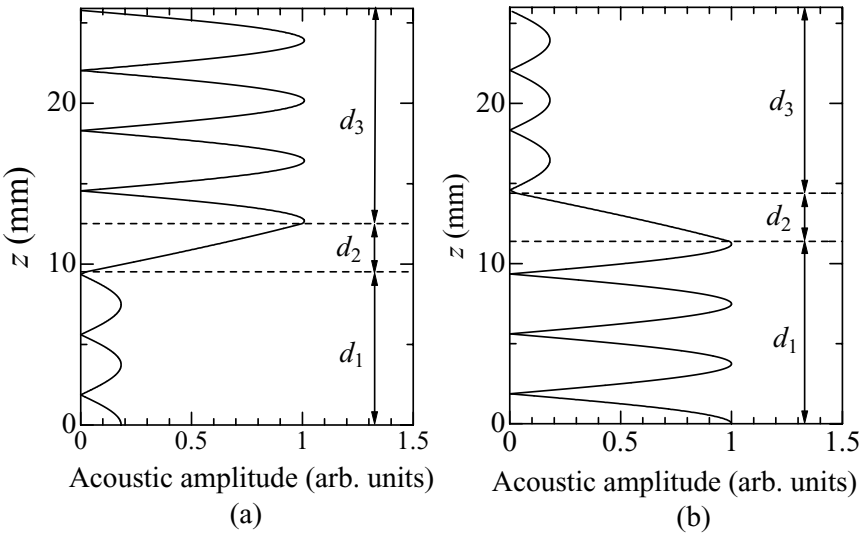
z (mm)
20
10
0
0
0.5
1
1.5
d_3
d_2
d_1
Acoustic amplitude (arb. units)
(a)
z (mm)
20
10
0
0
0.5
1
1.5
d_3
d_2
d_1
Acoustic amplitude (arb. units)
(b)

Fig. 2.

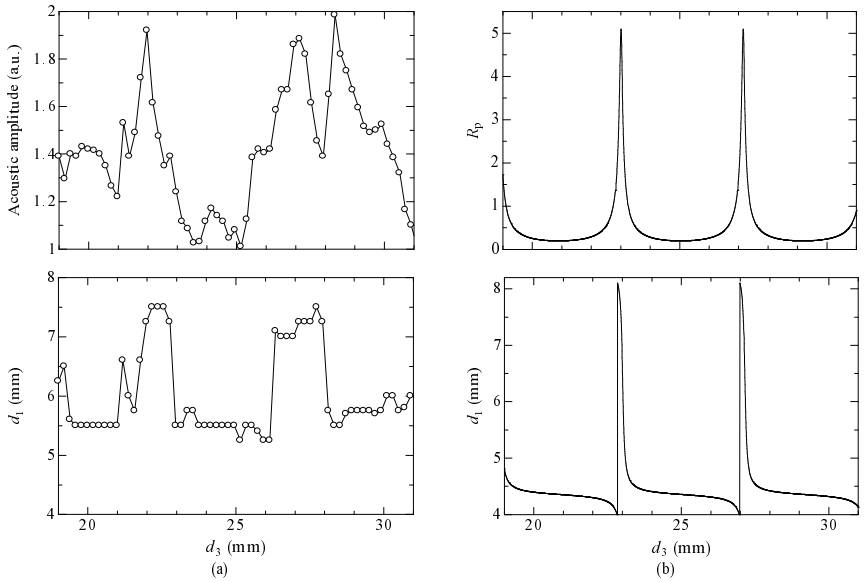

Fig. 3.

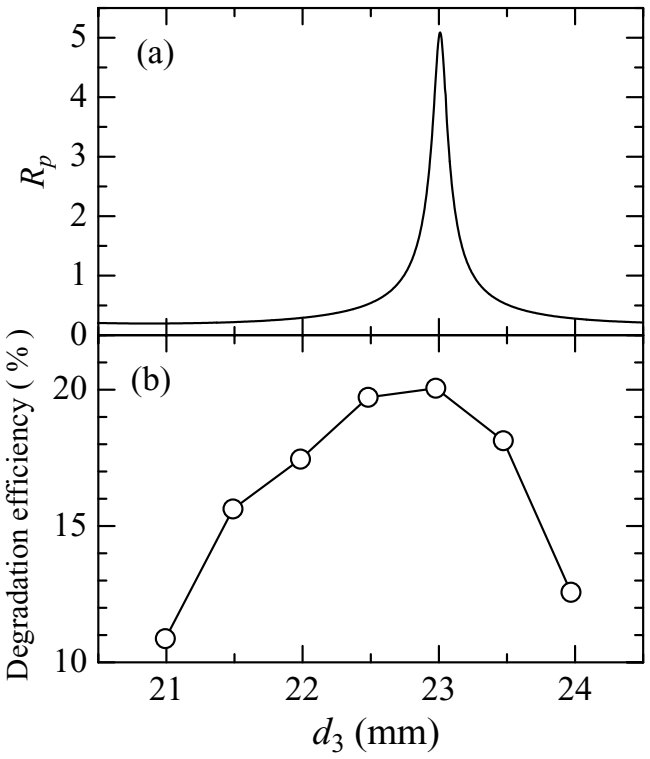

Fig. 4.

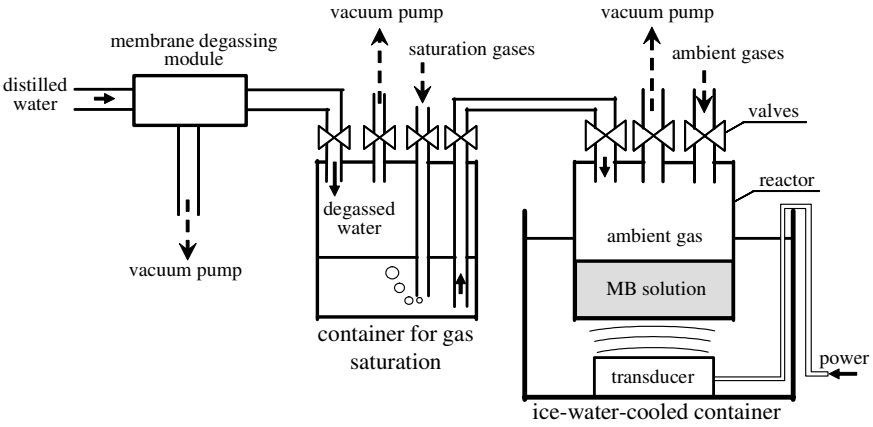
vacuum pump
vacuum pump
membrane degassing module
saturation gases
ambient gases
distilled water
valves
reactor
degassed water
ambient gas
vacuum pump
MB solution
container for gas saturation
power
transducer
ice-water-cooled container

Fig. 5.

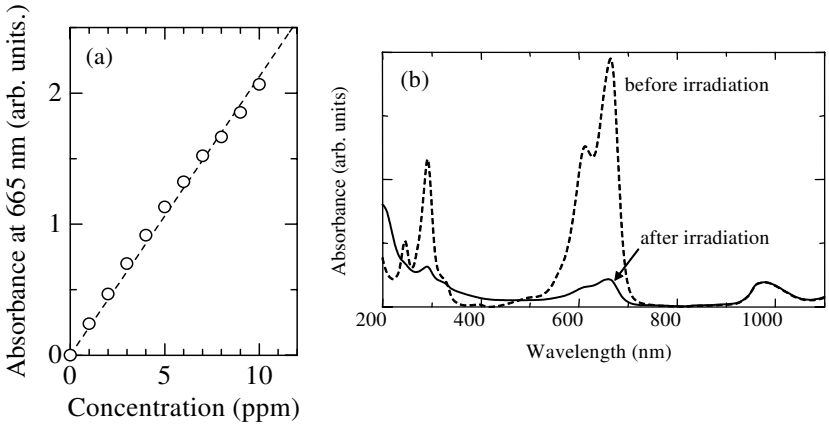
(a)
Absorbance at 665 nm (arb. units.)
Concentration (ppm)
0
1
2
0
5
10
(b)
before irradiation
after irradiation
Absorbance (arb. units)
Wavelength (nm)
200
400
600
800
1000

Fig. 6.

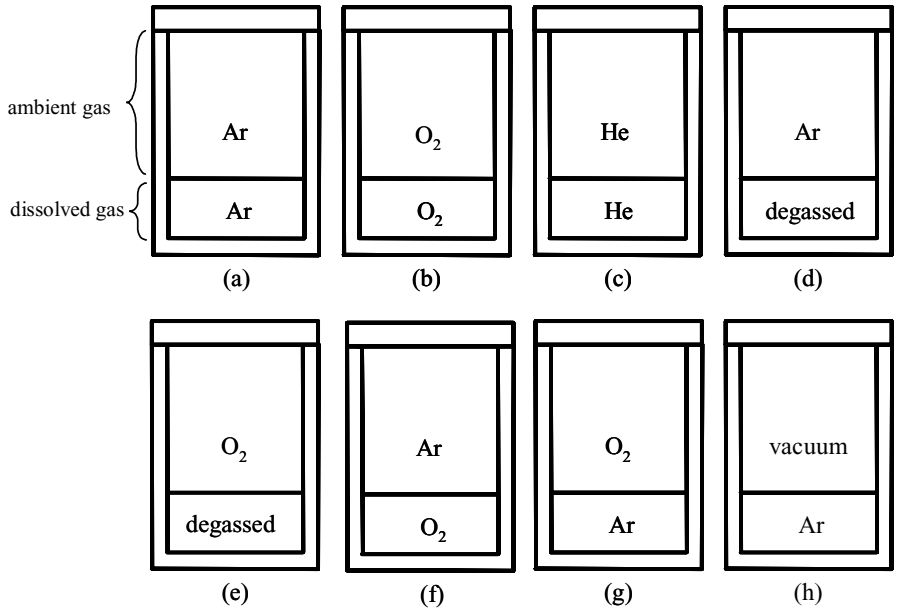
ambient gas
dissolved gas
Ar
Ar
(a)
O2
O2
(b)
He
He
(c)
Ar
degassed
(d)
O2
degassed
(e)
Ar
O2
(f)
O2
Ar
(g)
vacuum
Ar
(h)

Fig. 7.

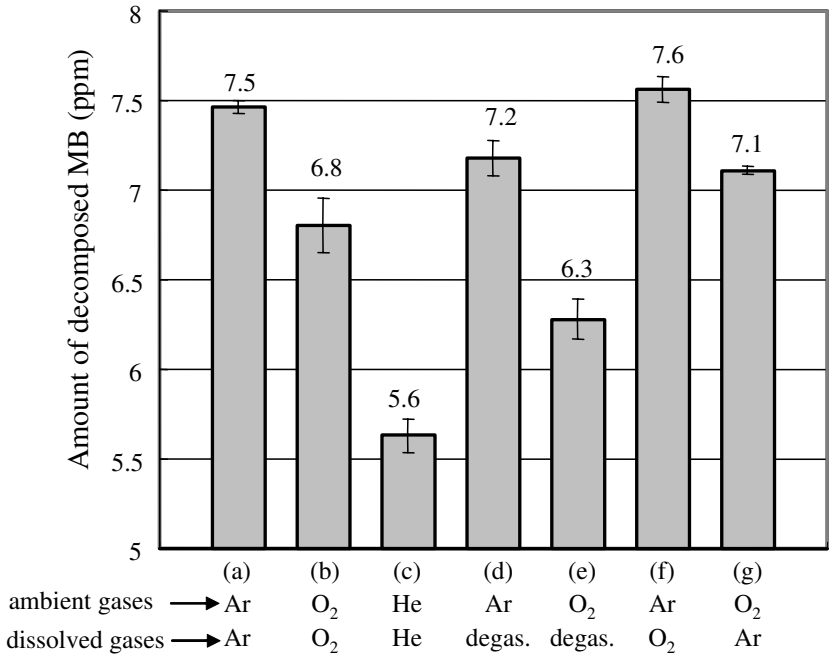
Amount of decomposed MB (ppm)
8
7.5
7
6.5
6
5.5
5
7.5
6.8
5.6
7.2
6.3
7.6
7.1
(a) (b) (c) (d) (e) (f) (g)
ambient gases → Ar O2 He Ar O2 Ar O2
dissolved gases → Ar O2 He He degas. degas. O2 Ar

Fig. 8.